*Journal of Chromatography*, 638 (1993) 119–135
Elsevier Science Publishers B.V., Amsterdam

CHROM. 24 944

# Options in electrolyte systems for on-line combined capillary isotachophoresis and capillary zone electrophoresis

Ludmila Křivánková* and Petr Gebauer

*Institute of Analytical Chemistry, Czech Academy of Sciences, Veveří 97, 611 42 Brno (Czech Republic)*

Wolfgang Thormann

*Institute of Clinical Pharmacology, University of Berne, Murtenstrasse 35, CH-3010 Berne (Switzerland)*

Richard A. Mosher

*Center for Separation Science, University of Arizona, Tucson, AZ 85721 (USA)*

Petr Boček

*Institute of Analytical Chemistry, Czech Academy of Sciences, Veveří 97, 611 42 Brno (Czech Republic)*

ABSTRACT

A theoretical description of the electrolyte systems that can be used in the on-line combination of isotachophoresis and zone electrophoresis is given. A classification of these systems is presented, based on the type of electrolyte used for the zone electrophoretic separation step. It is shown that transient sample stacking effects always persist from the isotachophoretic step to the beginning of the zone electrophoretic step and that they may negatively influence the zone electrophoretic separation and detection of the sample components. A mathematical description of these effects is given that allows the calculation of their magnitude and consequently the selection of operating conditions such that the stacking is decreased to an acceptable extent. In order to verify the reliability of the theoretical model, a modified PC simulation pack was prepared and used for investigating the behaviour of some model systems.

## INTRODUCTION

The rapidly developing method of capillary zone electrophoresis (CZE) suffers from some serious drawbacks. Some of them can be solved by improvements in the instrumentation used, but others are based on electrophoretic principles. High speed and high efficiency of the separations are achieved by performing the analyses in capillaries with very small inner diameters (0.02–0.01 mm) and injecting very small sample volumes of nanolitres and less. Although a concentration effect can occur at the beginning of the analysis when the sample passes the boundary with the background electrolyte (BGE) [1–5], the sample is diluted by various dispersive effects during the separation process. Therefore, it is advisable to inject a small but reproducible pulse with a high sample concentration. To avoid the dispersion caused by electromigration, the concentration of the sample is, however, recommended to be at least 100 times

* Corresponding author.

0021-9673/93/$06.00 

lower than the concentration of the BGE [1]. In practice this means that nanolitre volumes of the sample are injected hydrodynamically or electrokinetically [6,7]. Technical (exact volume) and principle-related (sample composition changes) drawbacks of these procedures often result in the reproducibility being insufficient for both qualitative and quantitative evaluation [8]. Typical sample concentrations are $10^{-4}$–$10^{-6}$ $M$, which means that the amount present in the zone is $10^{-13}$ mol and less. To increase the sensitivity, very sensitive detectors need to be used; to increase detectability, preconcentration techniques have to be applied.

The preconcentration techniques that can be used during the electrophoretic separation include stacking of the sample at the boundary between the sample zone and the BGE [9–12] and migration in the isotachophoretic (ITP) mode for a certain time due either to the composition of the sample creating ITP conditions for the migration [13,14] or to an ITP system being a constituent part of the BGE both in one capillary [15,16] or in two coupled capillaries [17–20]. The reported increase in sample concentration is about one order of magnitude. The most effective method is the on-line coupling of ITP with CZE where a $10^4$-fold concentration increase can be achieved, and this even for a component present in a $10^5$-fold excess [21,22]. It follows from the principle of the ITP method [23] that the sample zones migrating behind the leading zone are adjusted to its concentration. Usually, tens of microlitres of a sample either more or less concentrated than the leading electrolyte (LE) are injected. After the ITP separation, nanolitre or smaller volumes of about $10^{-2}$ $M$ sample zones can be expected for microcomponents the concentration of which in the sample was about $10^{-6}$ $M$ or less. These zones migrate as a stack between the leading electrolyte (LE) and the terminating electrolyte (TE) with permanently sharp boundaries between them. Such a stack of zones presents an ideal sampling situation for zone electrophoresis. Components of high concentration, the presence of which can cause problems in ZE separations, can be driven out of the separation system during the isotachophoretic stage where their qualitative and quantitative evaluation is reliably performed. In contrast, the detection of components in small amounts can be a problem whenever the zone length is shorter than the width of the detector cell [21,22]. Although such a problem can be solved by adding spacers of suitable mobilities [24], this solution is not simple.

The advantage of the combination of ITP and CZE has been verified practically on different occasions, including the determination of thiamine in blood [17], nitrophenols and amino acids labelled with 2,4-dinitrophenol [21], cyanogen bromide digest of cytochrome *c* [16], the coccidiocide halofuginone in feedstuff [22], *o*-phthaldialdehyde and fluorescein isothiocyanate derivatives of amino acids [19], fluorescein isothiocyanate derivative of angiotensin [20] and protein mixtures [15,18].

A theoretical description of the transition of isotachophoresis to zone electrophoresis can be found in papers by Beckers and Everaerts [25,26] and Gebauer *et al.* [4]. However, no description of processes proceeding during the transition and the way in which they affect the proper zone electrophoretic migration could be found, although some attempts to characterize the ITP–CZE combination with respect to the electrolyte systems applied were reported [15,17,22]. It has been shown that in both ITP and CZE the selection of electrolyte systems in which the separation proceeds is of basic significance [27,28]. It is the composition of the LE [29] (and sometimes also of the TE [30]) in ITP and the BGE in CZE that directly influences the selectivity and separation efficiency [8,31]. In the ITP–ZE combination the proper selection of both electrolyte systems is obviously more difficult if they have to be chosen so that the advantages of both methods are complemented.

This study was aimed at providing a general classification of electrolyte systems applicable for the ITP–ZE combination, a theoretical description of the transition of the zones from the ITP mode to the ZE mode and definition of the conditions for the proper application of the method. A computer simulation program is used to illustrate the behaviour of sample zones in various electrolyte systems.

## EXPERIMENTAL

For computer simulations, the Arizona model [32,33] in its PC-adapted version [34] was executed on an Excel 486 computer (Walz Computer, Berne, Switzerland) running at 50 MHz. The initial conditions for a simulation which must be specified include the distribution of all components, the p$K$ and mobility values of the buffer and sample constituents, the current density and the duration of the current flow, and also the column length and the segmentation. The program outputs concentration, pH and conductivity profiles as functions of time. A conversion program was written that allows the use of a specified slice of a computer-simulated ITP pattern and also the specification of the buffers on either side of the selected region, as the starting distribution for the CZE step.

For the example given in this work, a 10-cm column containing 400 segments was employed. For ITP, a leader composed of 0.01 $M$ HCl and 0.02 $M$ histidine and a terminator containing 0.01 $M$ of a strong acid T (mobility of $25 \cdot 10^{-9}$ $m^2$ $V^{-1}$ $s^{-1}$) and 0.02 $M$ histidine were employed. The input data are given in Table I. For this configuration, the composition of the adjusted terminator was calculated to be 0.00693 $M$ T and 0.01695 $M$ histidine. Two strong acids were chosen as sample components. For the simulation of the BGE–S–BGE system (S = sample), a background electrolyte consisting of 0.02 $M$ histidine and 0.008 $M$ of a strong acid (mobility $35 \cdot 10^{-9}$ $m^2$ $V^{-1}$ $s^{-1}$) was used. The current density and total running time were 20 A $m^{-2}$ and 25 min, respectively. For the simulations of the second (CZE) step, the slice between mesh points 206 and 236 of the 25-min ITP time point having a length of 6.75 mm was chosen. Of this length, *ca.* 3.8 mm ($l_L^*$, see below) were occupied by the leading zone and *ca.* 2.15 mm ($l_T$, see below) by the adjusted terminating zone. The position of the left boundary of this ITP column slice introduced as the sample for the consecutive CZE run was shifted to a 0.5 cm column length prior to application of current (100 A $m^{-2}$).

TABLE I

ELECTROCHEMICAL PARAMETERS USED FOR SIMULATION [33]

| Compound | p$K_1$ | p$K_2$ | Mobility ($10^9$ $m^2$ $V^{-1}$ $s^{-1}$) |
|---|---|---|---|
| Histidine | 6.04 | 9.17 | 20.2 |
| $Cl^-$ | | | 79.1 |
| T | | | 25.0 |
| Sample A | | | 40.0 |
| Sample B | | | 30.0 |
| $H^+$ | | | 362.7 |
| $OH^-$ | | | 198.7 |

## RESULTS AND DISCUSSION

### *Classification of electrolyte systems used in combined ITP–CZE*

In principle there are three ways of performing an ITP–CZE combination technique as far as the electrolyte system is concerned, as follows.

*T–S–T system (Fig. 1a):* the simplest way is to use the terminating electrolyte as the background electrolyte (BGE) for CZE. Here, the preseparation capillary is filled with the leading and terminating electrolytes and the analytical capillary is filled with the terminating electrolyte. In the first stage, the sample is injected in

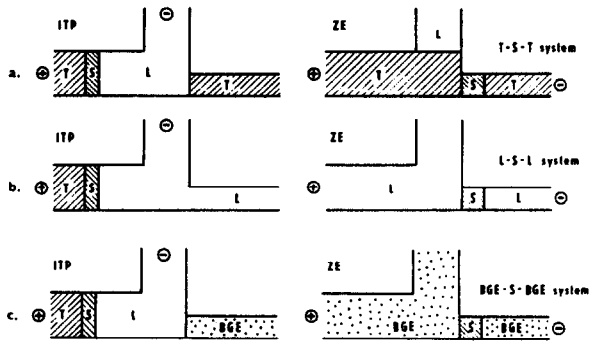


Fig. 1. Classification of electrolyte systems used in the on-line combination of ITP and ZE. The left panel shows the situation in the preseparation capillary at the end of the isotachophoretic separation. The right panel shows the situation in the analytical capillary at the beginning of the zone electrophoretic separation for (a) the terminating electrolyte (T), (b) the leading electrolyte (L) and (c) another background electrolyte (BGE) being used as the electrolyte for the separation by zone electrophoresis. S = Sample zone. The depicted schemes relate to cationic analyses: by changing polarity they apply to anionic systems.

between the leading and terminating electrolytes, current is switched on and passes between the terminating and auxiliary electrodes only through the preseparation capillary. The components of the sample form consecutive isotachophoretic zones with sharp boundaries, arrange themselves in order of decreasing mobilities and change their concentrations depending on the concentration of the leading zone. Before the stack of analytes reaches the bifurcation point between the preseparation and analytical capillaries, the current is switched to the analytical capillary (right panel of Fig. 1a). The ITP stack now becomes the sample for the CZE analysis.

*L–S–L system (Fig. 1b):* in the second approach, the leading electrolyte is employed as the BGE. In this instance, when the stack of isotachophoretically arranged zones of analytes reaches the bifurcation point, the current is switched and the migration of analytes proceeds continuously into the analytical capillary. After the last analyte of the stack has entered the analytical capillary, the current is switched off and the terminating electrolyte within the preseparation capillary is flushed out and replaced with the leading electrolyte. Then the current is again applied (right panel of Fig. 1b).

*BGE–S–BGE system (Fig. 1c):* The third possibility is to use a BGE different from LE or TE. The procedure is similar to the L–S–L system: after the current has been switched off, the terminating electrolyte is replaced by the BGE.

*T–S–T system*

We shall now describe in more detail the first of the systems under consideration (see Fig. 1a). Here the T–S–L stack migrates into the bifurcation block and, after the entire leading zone has migrated to the helping electrode, the electric current is switched off to the analytical electrode and the sample zones are separated zone electrophoretically in the terminating electrolyte. The second panel of Fig. 1a shows this ideal case where the switch-over was performed at the right moment when the leading zone had just migrated out of the preseparation capillary so that only the stack of the sample zones but no leading ion were introduced into the analytical capillary. In practice, however, it is necessary to perform this switching over earlier in order not to lose part of the sample owing to outflow to the auxiliary electrode. Hence some amount of the leading ion is always introduced into the analytical capillary together with the sample. The distance of the tell-tale detector from the end of the preseparation capillary determines the maximum volume of the leading zone which may pass to the analytical capillary because the switching over is usually not performed earlier than the first sample zone reaches the tell-tale detector.

Let us start the description with the just-mentioned time point when the stack of the sample zones is caught by the tell-tale detector. Fig. 2 shows the notation used. In the preseparation capillary (denoted capillary 3), the stack from the ITP step is present. The leading electrolyte zone contains the leading ion L at a concentration $c_{L,3}$ and the common counter ion R; the conductivity of this zone is $\kappa_3$. The analytical capillary (capillary 1) is filled with the terminating electrolyte; it contains the terminating ion T at a concentration $c_{T,1}$ and its conductivity is $\kappa_1$. All ions are assumed to be strong electrolytes,

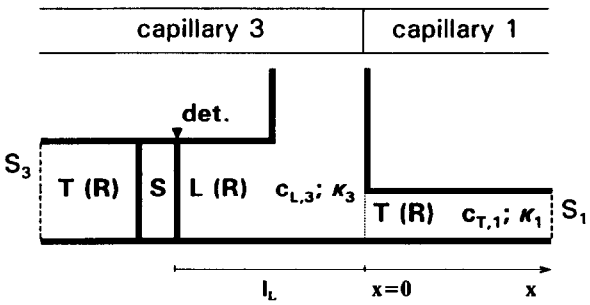


Fig. 2. Scheme of the interface between the preseparation (3) and analytical (1) capillaries serving for the separation in isotachophoretic and zone electrophoretic modes, respectively, in the T–S–T electrolyte system. The situation is depicted at the moment when the sample zone migrating in the ITP mode reaches the tell-tale detector in the preseparation capillary. This capillary of inner cross-section $S_3$ contains terminating (T) and sample (S) zones adjusted to the leading ion (L) of the concentration $c_{L,3}$ and the common counter ion R. The conductivity in the leading zone is $\kappa_3$. The analytical capillary of inner cross-section $S_1$ is filled with the terminating electrolyte, the concentration and conductivity of which are $c_{T,1}$ and $\kappa_1$, respectively. The zero point on the longitudinal axis is positioned at the interface between the capillaries; the length of the leading zone in the preseparation capillary, which will be introduced into the analytical capillary, is $l_L$.

except the counter ion, which is a weak electrolyte. The cross-sections of the analytical and preseparation capillary are $S_1$ and $S_3$, respectively. The one-dimensional coordinate system is positioned so that the origin ($x = 0$) lies at the interface of the preseparation and analytical capillaries. The time count starts ($t = 0$) at the time of switching over to the analytical electrode; it is assumed that the length of the leading zone still present in the preseparation capillary is $l_L$ at this time point. The separation system is assumed to have closed capillaries, *i.e.*, without electroosmotic flow.

The description of the processes that take place in the analytical capillary must be divided into several steps. In the first, which proceeds from the starting situation (Fig. 3a), the leading zone migrates into the analytical capillary, its concentration being readjusted to the Kohlrausch value [31] corresponding to the parameters of the terminating zone. The migration velocity of its rear boundary (equal to the isotachophoretic velocity in capillary 3) is $i_3 u_L/\kappa_3$ ($i_3$ is the electric current density in capillary 3 and $u_L$ is the mobility of ion L) and the time when the entire zone of L had migrated into the analytical capillary is thus given by

$$t_0 = l_L \cdot \frac{\kappa_3}{i_3 u_L} = l_L^* \cdot \frac{\kappa_3}{i_1 u_L} \quad (1)$$

where $l_L^* = l_L S_3/S_1$ is the length of the leading zone in capillary 3 reduced to the cross-section of capillary 1. This is also the time when the sample zones start to enter the analytical capillary (see Fig. 3b).

As was shown previously [35], the front boundary of the leading zone penetrating into the terminating zone is a diffuse one. This diffuse part becomes longer with time, which results in the disappearance of the (isotachophoretic) concentration plateau of the leading zone (Fig. 3c) at the time [4]

$$t_d = l_L^* \cdot \frac{\kappa_3}{i_1 (u_L - u_T)} \quad (2)$$

and at the position $x_d$.

At this time, all the sample components that migrated isotachophoretically in capillary 3 are still migrating in stack at the (self-sharpening) rear boundary of the L zone. Since this moment

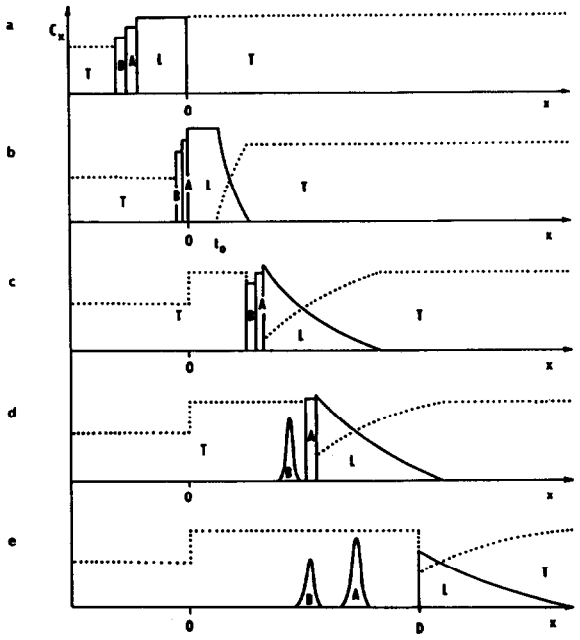


Fig. 3. Scheme of transition of the stack of zones from isotachophoretic migration to zone electrophoretic movement in the T–S–T electrolyte system. The situations are shown at the following time moments: (a) $t = 0$, when the current is switched to the analytical capillary; (b) $t_0$, when the entire zone of the leader electrolyte has just migrated into the analytical capillary; (c) $t_d$, when the ITP concentration plateau of the leading zone has just disappeared; (d) when the zone B has destacked while A is still migrating in the stack; (e) $t_{z,t}$, when all the sample zones migrate in zone electrophoretic mode and the rear boundary of the leading zone just passes the detector, thus opening the time window for detection. L = Leading electrolyte; T = terminating electrolyte; A, B = sample zones; $x$ = longitudinal coordinate; $c_X$ = concentration of a component in the separation system; 0 = interface between the analytical and preseparation capillaries; D = position of the detector.

they are gradually destacked in order of their increasing mobilities (Fig. 3d); the destacking time of a component X is given by [4]

$$t_{X,e} = t_d \left( \frac{u_L - u_T}{u_L - u_X} \right)^2 \quad (3)$$

The longitudinal coordinate where this destacking proceeds is given by [4]

$$x_{X,e} = t_d \cdot \frac{i_1}{\kappa_1} \left( \frac{u_L - u_T}{u_L - u_X} \right)^2 \frac{u_X^2}{u_L} \quad (4)$$

By substituting $t_d$ from eqn. 2, expressing the specific conductivities by $\kappa_3/\kappa_1 = c_{L,3}(u_L + u_R)/$

$c_{T,1}(u_T + u_R)$ and by using the Kohlrausch equation [31] in the form $c_{L,1} = c_{T,1}u_L(u_T + u_R)/u_T(u_L + u_R)$, we obtain

$$x_{X,e} = l_L^* \cdot \frac{c_{L,3}}{c_{L,1}} \cdot \frac{p_{L,T}}{p_{L,X}^2} \quad (5)$$

where $p_{ij} = u_i/u_j - 1$ [36] is the selectivity between components $i$ and $j$. From eqn. 5, it follows that the destacking coordinate of component X depends on the amount of the leading electrolyte introduced into the analytical capillary, on the ratio of concentration readjustment at the interface between both capillaries and on the selectivity between the leading component and component X.

Only after the sample components have been destacked can their zone electrophoretic migration and separation start (Fig. 3e). A general condition can therefore be formulated that the destacking of all components must proceed before they pass the detector, *i.e.*, $x_{X,e} < x_r$, where $x_r$ is the position of the detector in the analytical capillary. The time window for the detection of the sample components starts by the time $t_{z,r}$ when the rear boundary of the L zone passes through a fixed-point detector (Fig. 4). For this time it follows that [4]

$$t_{z,r} = \frac{\kappa_1}{i_1 u_L}\left(\sqrt{x_r} + \sqrt{x_d} \cdot \frac{u_L - u_T}{u_T}\right)^2 \quad (6)$$

In order to obtain complete destacking, for the detection time of the first (fastest) sample component A it must hold that $t_{A,r} \geq t_{z,r} + 4^t\sigma_A$,

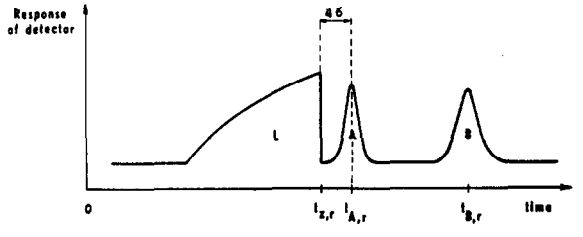


Fig. 4. Record of completely destacked sample components A and B during the separation in the T–S–T electrolyte system. In contrast to Fig. 3, where the concentration profile of the leader shows a concave shape, the respective profile as a function of time is convex here [37]. $t_{z,r}$, $t_{A,r}$ and $t_{B,r}$ are the detection times of the rear boundary of the leading zone and of the sample zones A and B, respectively.

where $^t\sigma_A$ is the time-based variance of the concentration profile of zone A. The detection time of any component X is given by [4]

$$t_{X,r} = x_r \cdot \frac{\kappa_1}{i_1 u_x} + t_d \cdot \frac{(u_L - u_T)^2}{(u_L - u_X)u_L} \quad (7)$$

Evidently, with increasing mobility of a component X, both its detection time $t_{X,r}$ and its destacking time $t_{X,e}$ become close to $t_{z,r}$. The mobility value of the component that would be destacked just when passing through the detector can thus be obtained by setting $t_{z,r} = t_{X,e}$ from eqns. 3 and 6:

$$u_{X,max} = \frac{u_L}{1 + \sqrt{\frac{l_L^*}{x_r} \cdot \frac{\kappa_3}{\kappa_1} \cdot \frac{u_L - u_T}{u_L}}} \quad (8)$$

Fig. 5 shows the calculated dependence of $t_{X,r}$ *vs.* $u_X$ for a model system and for three detection distances $x_r$. Each curve consists of two parts. The linear part (for high $u_X$ values) represents the $t_{z,r}$ value which is independent of $u_X$; it indicates that the substances have not left the

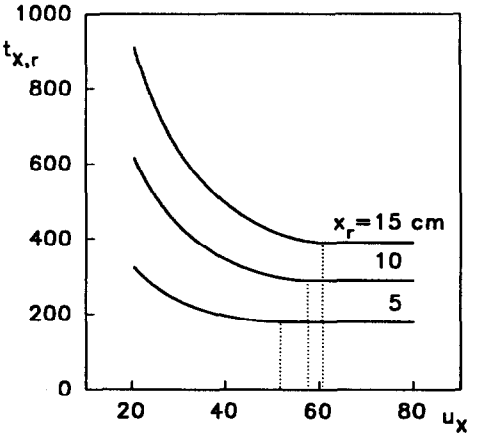


Fig. 5. Calculated dependence of the detection time of a substance X ($t_{X,r}$) on the mobility of this substance ($u_X$) (in $10^{-9}$ m$^2$ V$^{-1}$ s$^{-1}$) for three different positions of the detector, $x_r$, in the T–S–T electrolyte system. Dotted lines designate the mobility of the component that has destacked just when passing the detector, $u_{X,max}$. For $u_X > u_{X,max}$ the sample zones are still migrating in stack when passing the detector whereas for $u_X < u_{X,max}$ they migrate already in the electrophoretic mode. The values used for calculation were $u_L = 80 \cdot 10^{-9}$ m$^2$ V$^{-1}$ s$^{-1}$, $u_T = 20 \cdot 10^{-9}$ m$^2$ V$^{-1}$ s$^{-1}$, $u_R = 40 \cdot 10^{-9}$ m$^2$ V$^{-1}$ s$^{-1}$, $l_L^* = 0.01$ m, $c_{L,3} = c_{T,1} = 0.01$ $M$, $i = 500$ A m$^{-2}$.

stack yet when passing the detector. For $u_X < u_{X,max}$, the curve rises as $u_X$ decreases, which corresponds to sample zones passing the detector already destacked and later than the (stack at the) sharp rear boundary of the L zone.

From the above, it follows that it is desirable to keep the destacking times of all components as short as possible. The possibilities follow directly from the comment after eqn. 5. The major and most straightforward possibility for suppressing the sample stacking in the analytical capillary is to keep the length of the L zone introduced into the analytical capillary as short as possible. This can be achieved either by decreasing the length of the leading zone in the preseparation capillary at the moment of current switching or by increasing the readjustment ratio at the interface of both capillaries, *viz.*, by increasing the electrolyte concentration in the analytical capillary, $c_{T,1}$. The effect of both these parameters on the destacking distance $X_{X,r}$ can be clearly seen from Fig. 6 calculated for a model system.

The possibilities of decreasing the amount of the leader introduced are limited, however, and depend on the instrumentation used. Therefore, the other possibility must be taken into account, consisting in increasing the selectivity between the leading component and the sample components under investigation. As follows from eqn. 5, $x_{X,e}$ is indirectly proportional to the square of $p_{L,X}$ so that it can be decreased very effectively by selecting a leader of sufficiently high mobility. Fig. 7 shows how the value of $x_{X,e}$ decreases with increasing the value of $u_L - u_X$ and reveals the group of sample components that will be still migrating in stack when passing a fixed-point detector (see the parts of the curves above the dashed line when $x_r < x_{x,e}$).

Fig. 8 illustrates the theory by an example of a computer-simulated system. Fig. 8a shows the simulation of the first step resulting in rectangular concentration profiles as is usual in ITP. In Fig. 8b, the evolution of the concentration profiles in the analytical capillary is shown. At the beginning we can see very sharp peaks still migrating in the transient ITP stack, whereas dispersion of the zones appears whenever they leave the stack and migrate in the ZE mode. The

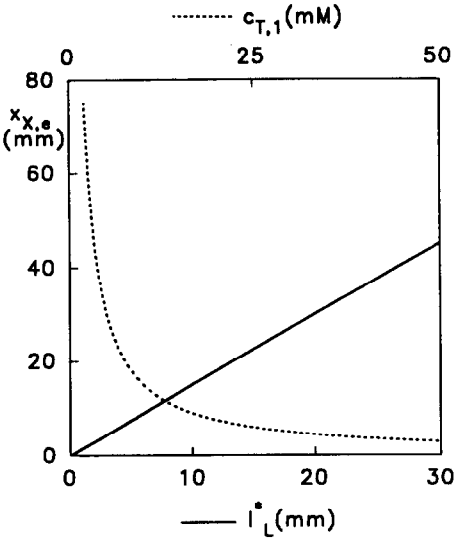


Fig. 6. Calculated dependence of the destacking distance of a sample zone ($x_{X,e}$) on the length of the leading zone cut into the analytical capillary ($l^*_L$, full line) and on the concentration of the terminator used as the BGE in the analytical capillary ($c_{T,1}$, dashed curve) in the T–S–T electrolyte system. The values used for calculation were $u_L = 80 \cdot 10^{-9}$ $m^2$ $V^{-1}$ $s^{-1}$, $u_T = 20 \cdot 10^{-9}$ $m^2$ $V^{-1}$ $s^{-1}$, $u_R = 40 \cdot 10^{-9}$ $m^2$ $V^{-1}$ $s^{-1}$, $u_X = 40 \cdot 10^{-9}$ $m^2$ $V^{-1}$ $s^{-1}$. The first dependence was calculated using $l^*_L = 0.01$ m; for the second, the concentration $c_T = 0.01$ *M* was chosen.

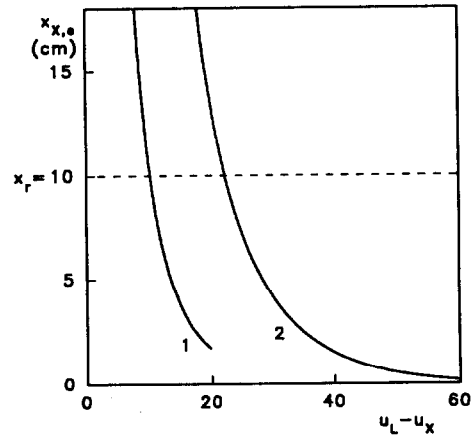


Fig. 7. Calculated effect of the difference between leading and sample mobilities ($u_L - u_X$) (in $10^{-9}$ $m^2$ $V^{-1}$ $s^{-1}$) on the distance where destacking proceeds ($x_{X,e}$) for two model examples. The intersection of the dependence with the position of the detector designates the group of substances that are not destacked prior to their passage through the detector (parts of the curves above the dashed line). For the values used for calculation, see Table I.

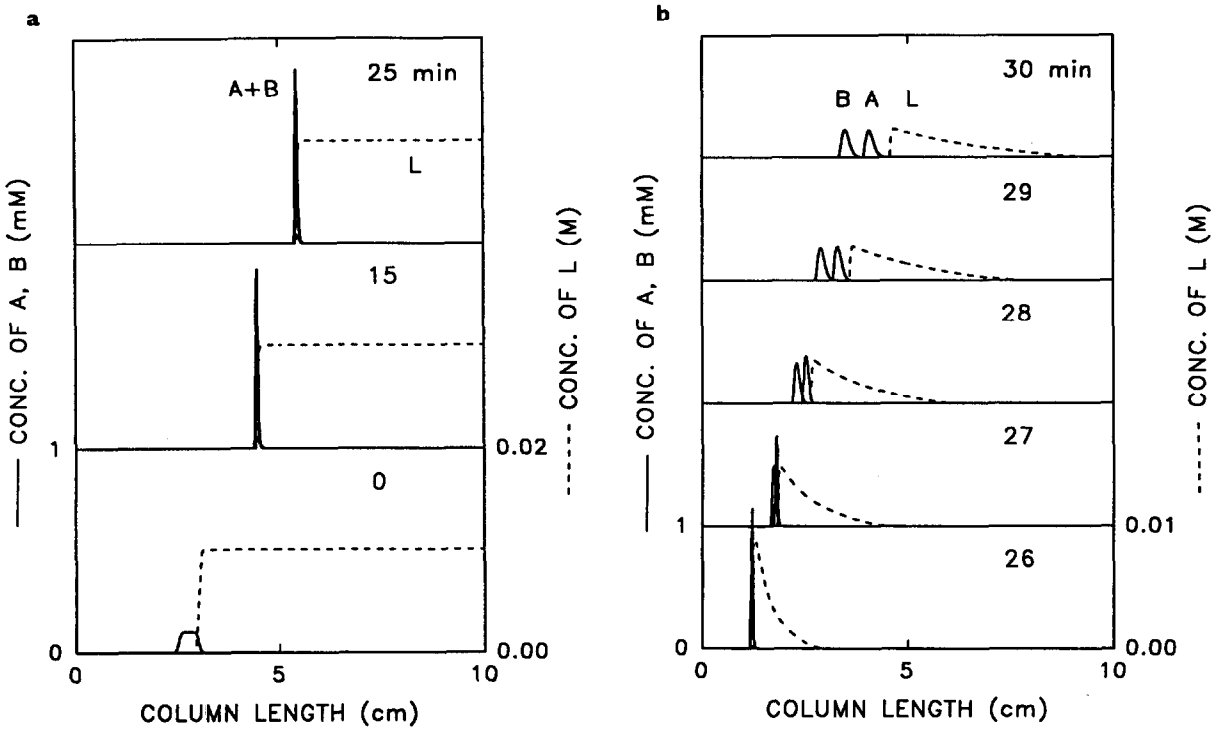


Fig. 8. Computer simulation of the separation of a pair of analytes A and B by the ITP–ZE combination in the T–S–T system. (a) Isotachophoretic step; (b) zone electrophoretic step. The concentration profiles shown correspond to the denoted time intervals. The values used for calculations were $u_L = 80 \cdot 10^{-9}$ m$^2$ V$^{-1}$ s$^{-1}$, $u_T = 25 \cdot 10^{-9}$ m$^2$ V$^{-1}$ s$^{-1}$, $u_R = 30 \cdot 10^{-9}$ m$^2$ V$^{-1}$ s$^{-1}$, $u_A = 40 \cdot 10^{-9}$ m$^2$ V$^{-1}$ s$^{-1}$, $u_B = 30 \cdot 10^{-9}$ m$^2$ V$^{-1}$ s$^{-1}$, $l_L^* = 6.75 \cdot 10^{-3}$ m, $c_T = 0.0069$ $M$, $c_R = 0.0169$ $M$, $i$ = (a) 20 and (b) 100 A m$^{-2}$.

destacking times calculated from eqn. 3 (27.2 min for component A and 26.4 min for component B) agree well with the simulation result.

*L–S–L system*

In the second type of electrolyte combination, the first stage of the separation proceeds just in the same way as in the T–S–T system (Fig. 1b); the difference is that the analytical capillary is filled with the leading electrolyte. After the current has been switched over and the sample zones have migrated into the analytical capillary (for the ideal case, see the second panel in Fig. 1b), the analysis is stopped and the contents of the preseparation capillary are filled with leading electrolyte as well. Then the analysis is continued.

Fig. 9 shows the starting situation of this second step as it corresponds to current practice where, together with the sample zones, some

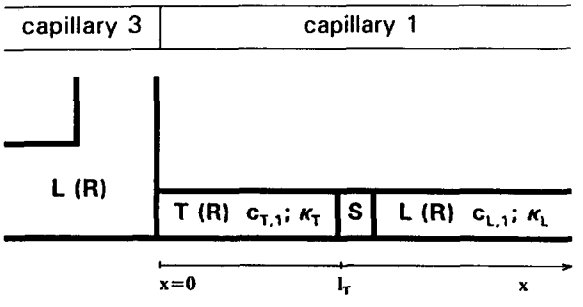


Fig. 9. Scheme of the interface between the preseparation and analytical capillaries serving for the separation in isotachophoretic and zone electrophoretic modes, respectively, in the L–S–L electrolyte system. The situation is depicted at the moment when the current is switched on across both capillaries after the terminator (T) in the preseparation column has been replaced by the leading (L) electrolyte. The concentration of T, $c_{T,1}$, is Kohlrausch-adjusted according to $c_{L,1}$; the conductivities in zones T and L are $\kappa_T$ and $\kappa_L$, respectively. The zero point on the longitudinal axis is positioned at the interface between the capillaries; the length of the terminating zone cut into the analytical capillary is $l_T$.

amount of the terminator has been introduced into the analytical capillary (see also Fig. 10a). This terminating zone of length $l_T$, with its concentration $c_{T,1} = c_{T,3}$ adjusted to the concentration of the leader ($c_{L,1} = c_{L,3}$), is necessary to ensure the quantitative transfer of all sample zones into the analytical capillary. This again leads to the unwanted stacking effects that have to be minimized.

A detailed mathematical description of this type of stacking has not been described previously; a simple way to derive the necessary equations is shown below. The resulting relationships are similar to those for stacking by the leading substance.

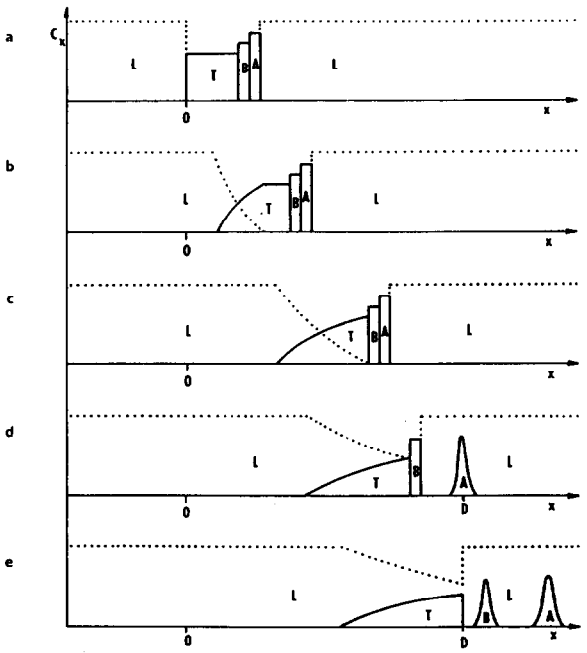


Fig. 10. Scheme of transition of the stack of zones from isotachophoretic migration to zone electrophoretic movement in the L–S–L electrolyte system. The situations are shown at the following time moments: (a) $t = 0$, when the current is again switched on over the system of both capillaries after the terminator (T) in the preseparation capillary was replaced with the leading electrolyte (L) and the separation in the ZE mode starts; (b) $t > 0$, when an ITP plateau of zone T still exists; (c) $t_d$, when the pure zone of T has just disappeared and only the transition mixed zone of T and L is present; (d) $t_{A,r}$, when the zone A is already destacked and passes the detector while B is still migrating in the stack; (e) $t_{z,r}$, when both sample zones migrate in the zone electrophoretic mode and the front boundary of the T zone is just passing the detector. L = Leading electrolyte; T = terminating electrolyte; A, B = sample zones; $x$ = longitudinal coordinate; $c_x$ = concentration of a component in the separation system; 0 = interface between the analytical and preseparation capillaries; D = position of the detector.

At the beginning of the second stage of the separation after replacement of the electrolyte in capillary 3 (start of migration in capillary 1, $t = 0$), the front boundary of the terminator zone and also the T–S–L zone stack migrate still isotachophoretically and the velocities of all the sharp boundaries are equal and given by

$$v_{T\text{-}L} = i_1 \cdot \frac{u_T}{\kappa_T} = i_1 \cdot \frac{u_L}{\kappa_L} \tag{9}$$

The rear boundary of the zone of the terminator (L–T boundary) develops into a diffuse one which forms a growing region of concentration transitions of both substances T and L (see Fig. 10b). The velocities of the rear and front edges of this transition are equal to the velocities of a single ion T and L in the isotachophoretic zone L and T, respectively:

$$v_1 = i_1 \cdot \frac{u_T}{\kappa_L} \qquad v_2 = i_1 \cdot \frac{u_L}{\kappa_T} \tag{10}$$

The balance written for the velocity difference $v_2 - v_{T\text{-}L}$ and for $l_T$ provides the time when the isotachophoretic concentration plateau of zone T disappears (see Fig. 10c):

$$t_d = l_T \cdot \frac{\kappa_L}{i_1} \cdot \frac{u_T}{u_L(u_L - u_T)} \tag{11}$$

For times longer than $t_d$, the L–T boundary remains sharp although the isotachophoretic zone of component T no longer exists (Fig. 10d). Its velocity decreases with time and so does the concentration of component T at this boundary. From ref. 35 we obtain for the ascending concentration profile of T

$$c_{T,L\text{-}T} = \frac{c_{L,1}u_T}{u_L - u_T} \cdot \frac{u_L + u_R}{u_T + u_R}\left(1 - \sqrt{v_1 \cdot \frac{t}{x}}\right) \tag{12}$$

and for the descending concentration profile of L

$$c_{L,L\text{-}T} = \frac{c_{L,1}u_T}{u_L - u_T}\left(\sqrt{v_2 \cdot \frac{t}{x}} - 1\right) \tag{13}$$

and the conductivity of any point $x$ of this profile at time $t$ is thus given by

$$\kappa_{L-T} = \kappa_{L,1}\sqrt{v_1 \cdot \frac{t}{x}} \tag{14}$$

For the velocity of the front boundary of zone T at times $t > t_d$ we can then write

$$\frac{dx_z}{dt} = \frac{i_1 u_T}{\kappa_z} = \sqrt{v_1 \cdot \frac{x_z}{t}} \tag{15}$$

where the subscript $z$ relates to the parameters of the transition zone at this boundary. Rearrangement and integration of this equation from $x_d$ to $x$ and from $t_d$ to $t$ provides

$$\sqrt{x_z} = \sqrt{v_1 t} + \sqrt{x_d} \cdot \frac{u_L - u_T}{u_L} \tag{16}$$

The destacking process starts at time $t_d$; the destacking of a component X proceeds at the time $t_{X,e} > t_d$ when the velocity of the stacking front boundary of zone T has decreased so that it became equal to the velocity of free component X in the leading electrolyte, *i.e.*, $v_z = v_{X,L} = i_1 u_X / \kappa_L$:

$$\sqrt{v_1 \cdot \frac{x_z}{t_{X,e}}} = i_1 \cdot \frac{u_X}{\kappa_L} \tag{17}$$

Substitution from eqn. 16 and rearrangement provide the destacking time of component X:

$$t_{X,e} = t_d \left(\frac{u_L - u_T}{u_X - u_T}\right)^2 \tag{18}$$

Obviously the sample zone is stacked the longer the lower is its mobility. The destacking coordinate is obtained by introducing $t_{X,e}$ into eqn. 16:

$$x_{X,e} = t_d \cdot \frac{i_1}{\kappa_L}\left(\frac{u_L - u_T}{u_X - u_T}\right)^2 \frac{u_X^2}{u_T}$$

$$= l_T \cdot \frac{(u_L - u_T)u_X^2}{(u_X - u_T)^2 u_L} \tag{19}$$

From this equation it is seen that the destacking coordinate again depends on the length of the zone of the stacking component (here T) and on the mobilities of L, X and T. As we assume the same leader concentrations in both capillaries 1 and 3, there is no effect of the readjustment ratio, which is unity. In the opposite case, however, $l_T$ would of course involve this ratio also.

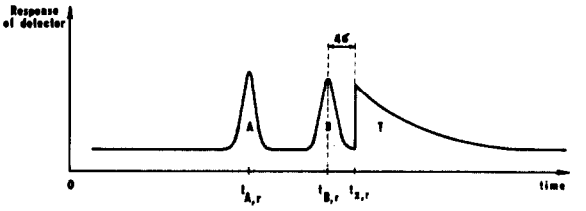


Fig. 11. Record of completely destacked sample components A and B during the separation in the L–S–L electrolyte system. In contrast to Fig. 10, where the concentration profile of the terminator shows a convex shape, the respective profile as a function of time is concave here [37]. $t_{z,r}$, $t_{A,r}$ and $t_{B,r}$ are the detection times of the front boundary of the terminating zone and of the sample zones A and B, respectively.

As already mentioned, the stacking is an effect which should be eliminated as only destacked zones can be separated in the zone electrophor-

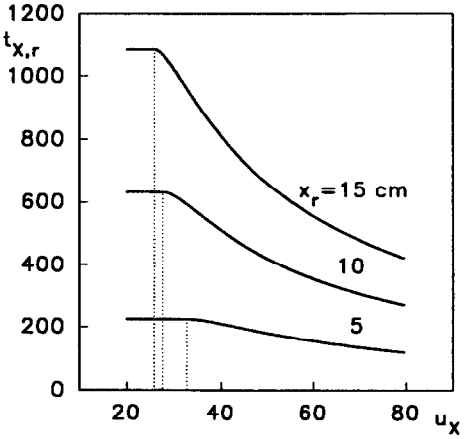


Fig. 12. Calculated dependence of the detection time of a substance X ($t_{X,r}$) on the mobility of this substance ($u_X$) (in $10^{-9}$ m$^2$ V$^{-1}$ s$^{-1}$) for three different positions of the detector, $x_r$, in the L–S–L electrolyte system. Dotted lines designate the mobility of the component that has destacked just when passing the detector, $u_{X,max}$. For $u_x < u_{X,max}$ the sample zones are still migrating in stack when passing the detector whereas for $u_X > u_{X,max}$ they migrate already in the electrophoretic mode. The values used for calculation were $u_L = 80 \cdot 10^{-9}$ m$^2$ V$^{-1}$ s$^{-1}$, $u_T = 20 \cdot 10^{-9}$ m$^2$ V$^{-1}$ s$^{-1}$, $u_R = 40 \cdot 10^{-9}$ m$^2$ V$^{-1}$ s$^{-1}$, $l_T = 0.01$ m, $c_L = 0.01$ *M*, $i = 500$ A m$^{-2}$.

etic mode and detected. For the detection time of component X it holds that

$$t_{X,r} = t_{X,e} + \frac{x_r - x_{X,e}}{v_{X,L}}$$

$$= x_r \cdot \frac{\kappa_L}{i_1 u_X} - t_d \cdot \frac{(u_L - u_T)^2}{(u_X - u_T)u_T} \quad (20)$$

which is a similar expression to eqn. 7.

Fig. 11 shows that a condition can be formulated for the slowest substance B which still is destacked before detection, *viz.*, $t_{B,r} \leq t_{z,r} + 4^t\sigma_B$. From the preceding section it follows that in the limiting case of the substance just being destacked when passing the detector not only $t_{X,r}$ and $t_{z,r}$ but also $t_{X,e}$ become equal. The respective mobility, $u_{X,min}$, thus can be obtained by combining eqns. 18 and 20:

$$u_{X,min} = \frac{u_T}{1 - \sqrt{\frac{l_T}{x_r} \cdot \frac{u_L - u_T}{u_L}}} \quad (21)$$

Fig. 12 shows, in analogy to Fig. 5, the calculated dependence of $t_{X,r}$ *vs.* $u_X$ for three detection distances $x_r$. Here the linear parts of the lines now correspond to low $u_X$ values of substances that have not left the stack yet when passing the detector. The respective values of $u_{X,min}$ are indicated by the dotted lines; for $u_X > u_{X,min}$, the curves fall as $u_X$ increases which corresponds to sample zones passing the detector already destacked and earlier than the (stack at the) sharp front boundary of the T zone.

As follows from eqns. 18 and 20, by increasing the length of the stacking zone (here expressed in the term of $t_d$; see eqn. 11), the destacking time of the sample zones is increased and their detection time is decreased as the substances are accelerated during their migration in stack. This is the opposite situation to that in the previous case where the stack retards the zones so that a longer zone of the stacking component (*i.e.*, longer destacking times) cause longer detection times. A comparison of both cases is shown in Fig. 13, where the dependences of the detection

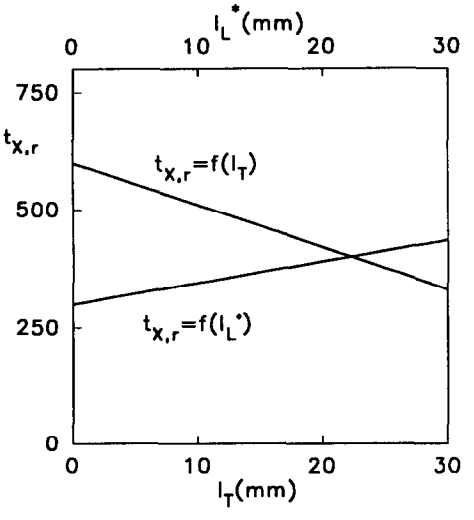


Fig. 13. Calculated dependence of the detection time on the length of the segment of zone L or T cut into the analytical capillary in the T–S–T or L–S–L electrolyte combination, respectively. The values used for calculation were $u_L = 80 \cdot 10^{-9}$ m$^2$ V$^{-1}$ s$^{-1}$, $u_T = 20 \cdot 10^{-9}$ m$^2$ V$^{-1}$ s$^{-1}$, $u_R = 40 \cdot 10^{-9}$ m$^2$ V$^{-1}$ s$^{-1}$, $u_X = 40 \cdot 10^{-9}$ m$^2$ V$^{-1}$ s$^{-1}$, $i = 500$ A m$^{-2}$, $x_r = 0.1$ m. For $t_{X,r} = f(l_L^*)$, $c_T = 0.01$ *M*; for $t_{X,r} = f(l_T)$, $c_L = 0.01$ *M*.

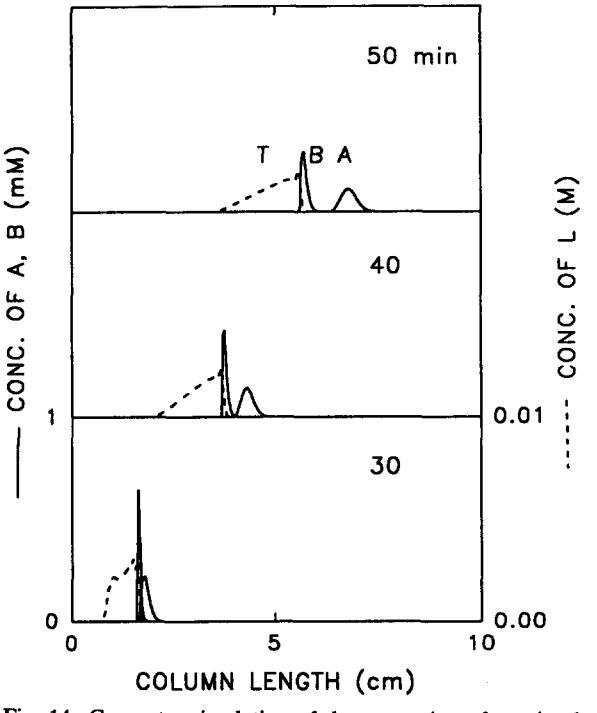


Fig. 14. Computer simulation of the separation of a pair of analytes A and B by the ITP–ZE combination in the L–S–L system. The isotachophoretic step was the same as shown in Fig. 8a. The concentration profiles shown correspond to the denoted time intervals. For the values used for calculations, see Table I.

time on the starting length of the stacking zone are calculated for the same model system.

Fig. 14 again illustrates the theory by a computer-simulated example with two sample components (A and B) and the stacking zone T. Here the mobility difference between B and T is three times lower than that between A and T, which causes much earlier destacking of component A (calculation using eqn. 18 provided the values 27.7 and 49.3 min for components A and B, respectively).

*BGE–S–BGE system*

The third system is the most general. Here, in the second step, the zone electrophoretic separation is performed in a background electrolyte that is different from both leader and terminator from the first step. First, after the sample zones have been detected by the tell-tale detector, the switch-over of the current to the analytical capillary is performed in the same way as was described for the T–S–T system. The remaining zone of the leader migrates into the analytical capillary, followed by the stack of the sample zones and the terminator. After some amount of the terminating zone has also migrated into the analytical capillary, the current is (in analogy to the L–S–L system) switched off, the preseparation capillary filled with the background electrolyte and the analysis continued (Fig. 1c). The behaviour of such a system and the way to

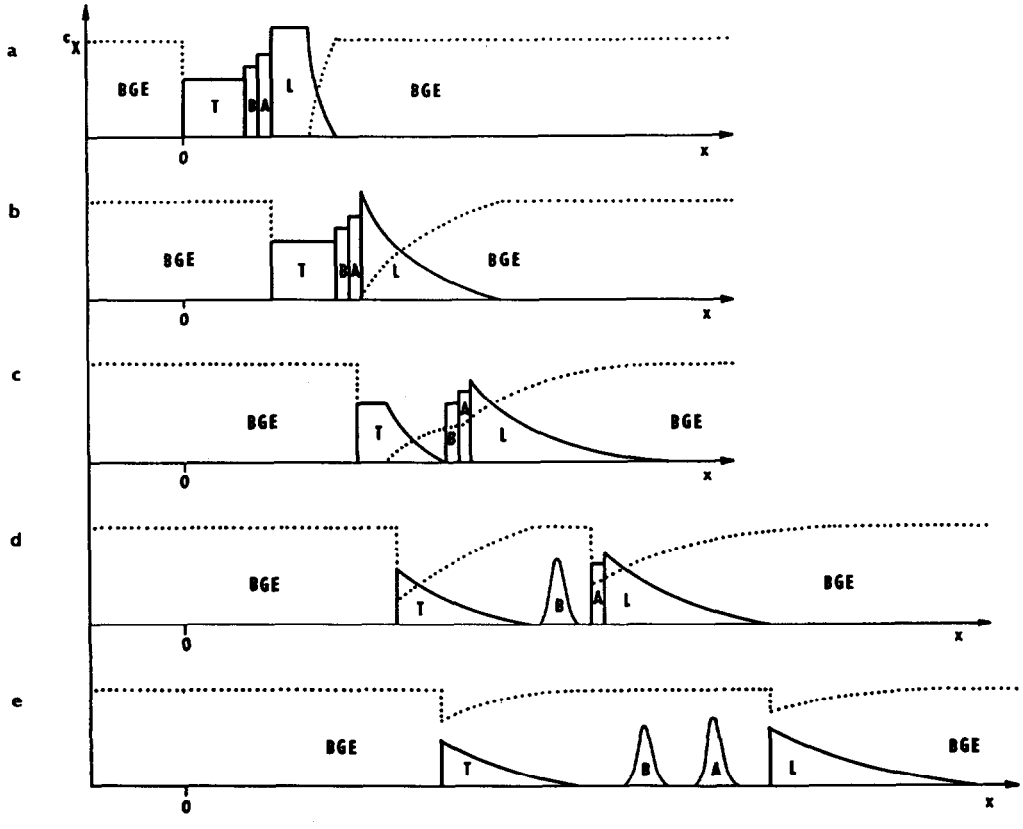


Fig. 15. Scheme of transition of the stack of zones from isotachophoretic migration to zone electrophoretic movement in the BGE–S–BGE electrolyte system for the case when the background electrolyte co-ion (BGC) possesses the lowest mobility of the system, $u_{BGC} < u_T < u_L$. The situations are shown at the time moments when: (a) the current is again switched on over the system of both capillaries after the terminator (T) in the preseparation capillary has been replaced with the BGE; the front boundary of zone L has already developed into a diffuse one; (b) the ITP concentration plateau of the L zone just disappeared; (c) the destacking of the T zone proceeds; (d) zones T and B have destacked while zone A is still migrating in stack behind L; (e) all the zones present in the BGE are destacked and migrating in the ZE mode. L = Leading electrolyte; T = terminating electrolyte; BGE = background electrolyte; A, B = sample zones; $x$ = longitudinal coordinate; $c_x$ = concentration of a component in the separation system; 0 = interface between the analytical and preseparation capillaries.

describe it depend on the mobility of the background electrolyte co-ion, $u_{BGC}$.

$u_{BGC} < u_T < u_L$. In this instance the system behaves similarly to the T–S–T system (Fig. 15). The background co-ion (BGC) is the slowest ion present and therefore the diffuse transition zone is started to be formed at the front boundary of the L zone which controls the migration of the zone stack (Fig. 15a). All other boundaries remain sharp, including the rear boundary of zone T. After the isotachophoretic plateau of zone L has disappeared and the BGE penetrates through the following zones, their destacking proceeds in the same way as described for the T–S–T system. First the zone of the terminator is destacked (Fig. 15c) and then the sample zones follow in order of increasing mobilities (Fig. 15d and e). For the calculation of the destacking time, destacking coordinate and detection time of a sample component X, eqns. 3, 5 and 7, respectively, can be used directly with the only change that the subscript T is replaced by BGC everywhere.

$u_T < u_L < u_{BGC}$. This arrangement resembles the L–S–L system (Fig. 16). The background electrolyte co-ion is the fastest ion and thus the diffuse transition is formed at the rear boundary of the terminating zone which plays the controlling role here (Fig. 16b). The destacking process starts with the zone of the highest mobility,

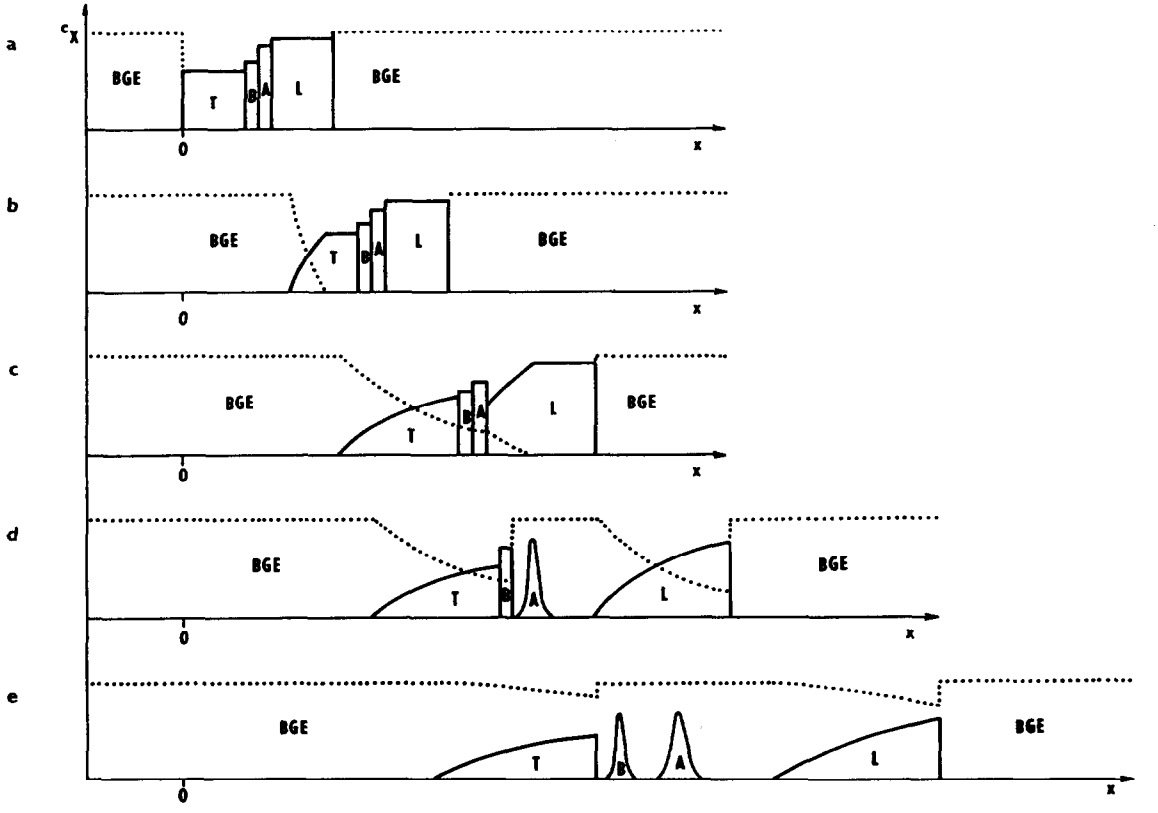


Fig. 16. Scheme of transition of the stack of zones from isotachophoretic migration to zone electrophoretic movement in the BGE–S–BGE electrolyte system for the case when the BGE co-ion (BGC) possesses the highest mobility of the system, $u_T < u_L < u_{BGC}$. The situations are shown at the time moments when: (a) the current is again switched on over the system of both capillaries after the terminator (T) in the preseparation capillary has been replaced with the BGE and zone electrophoretic separation starts; (b) an ITP plateau of zone T still exists; (c) the plateau of pure zone T has disappeared; (d) zones L and A have left the stack while zone B is still migrating in stack in front of T; (e) all the zones present in the BGE are destacked and migrating in the ZE mode. L = Leading electrolyte; T = terminating electrolyte; BGE = background electrolyte; A, B = sample zones; $x$ = longitudinal coordinate; $c_X$ = concentration of a component in the separation system; 0 = interface between the analytical and preseparation capillaries.

which is the L zone (Fig. 16c–e). For the calculation of the destacking time, destacking coordinate and detection time of a sample component X, eqns. 18, 19 and 20, respectively, can be used with the change that the subscript L is replaced by BGC everywhere. Note that these equations hold for the already readjusted zone of the terminator in capillary 1; its concentration and length must be calculated in a suitable way using the amount of terminator introduced into the analytical capillary and the Kohlrausch relationship.

$u_T < u_{BGC} < u_L$. This case represents a combination of the two previous ones (Fig. 17). The background electrolyte co-ion has an intermediate mobility. Both the front boundary of the L zone and the rear boundary of the T zone thus develop into diffuse transition zones (Fig. 17b and c). After the background co-ion has penetrated through the whole system, the zone stack splits into two separate parts, one being the L zone with a zone stack at its rear boundary and the other the T zone with a zone stack at its front boundary (Fig. 17d). The value of $u_{BGC}$ controls which of the two stacks a sample zone approaches: samples with $u_X > u_{BGC}$ stay at the

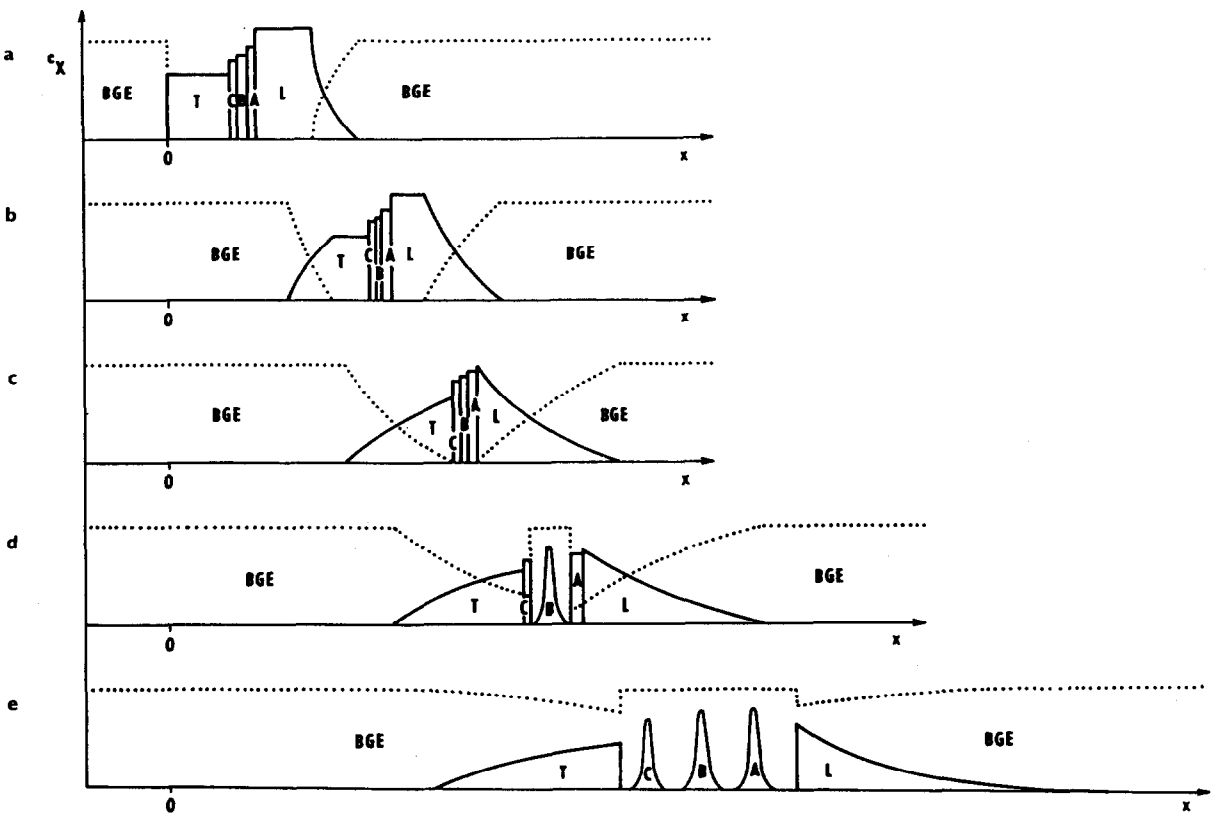


Fig. 17. Scheme of transition of the stack of zones from isotachophoretic migration to zone electrophoretic movement in the BGE–S–BGE electrolyte system for the case when the mobility of the BGE co-ion (BGC) is within the mobility of leader and terminator, $u_T < u_{BGC} < u_L$. The situations are shown at the time moments when: (a) the current is again switched on over the system of both capillaries after the terminator (T) in the preseparation capillary has been replaced with the BGE; the front boundary of zone L has already changed its sharp boundary into a diffuse one; (b) ITP plateaux of both zones L and T still exist; (c) the plateaux of pure zones T and L have disappeared; (d) zone B has left the stack and migrates zone electrophoretically while zones A and C are still migrating in stack behind L and in front of T, respectively; (e) all the zones present in the BGE are destacked and migrating in the ZE mode. L = Leading electrolyte; T = terminating electrolyte; BGE = background electrolyte; A, B, C = sample zones; $x$ = longitudinal coordinate; $c_X$ = concentration of a component in the separation system; 0 = interface between the analytical and preseparation capillaries.

L-zone stack and samples with $u_X < u_{BGC}$ stay at the T-zone stack. The destacking proceeds at each stack independently; at the L zone as it was described under $u_{BGC} < u_T < u_L$ and at the T zone as was described under $u_T < u_L < u_{BGC}$. Of course, in both instances the sample zones the mobilities of which are closest to the value of $u_{BGC}$ are destacked first.

Fig. 18 shows the dependence of the destacking coordinate on the mobility difference between the background co-ion and the sample ion for three different $u_{BGC}$ values. Note that the stacking effect becomes very pronounced when the difference is more than *ca.* $10 \cdot 10^{-9}$ m$^2$ V$^{-1}$ s$^{-1}$. Fig. 19 shows an illustration of such a combined system by computer simulation. Here the two sample substances were selected so that $u_A > u_{BGC}$ and $u_B < u_{BGC}$; this means that the destacking process of component A is controlled by component L and the destacking process of component B is controlled by component T. As $u_B$ is much closer to $u_T$ than $u_A$ is to $u_L$, B does not leave the stack as easily as does A. This is confirmed by the calculated destacking times,

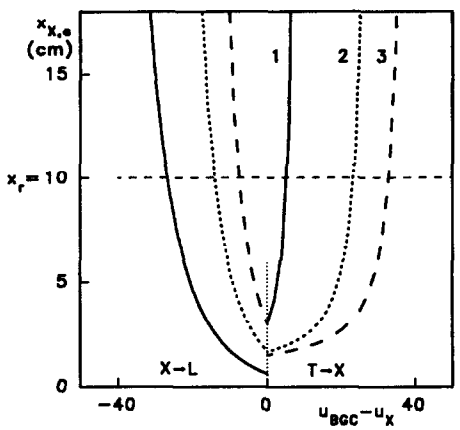


Fig. 18. Calculated dependence of the destacking distance of a sample zone ($x_{X,e}$) on the difference between its mobility and the mobility of background co-ion (in $10^{-9}$ m$^2$ V$^{-1}$ s$^{-1}$) in the BGE–S–BGE system from Fig. 17. For $u_X > u_{BGC}$, the system resembles the T–S–T system and L possesses the controlling role in destacking; for $u_X < u_{BGC}$, the system resembles the L–S–L system and T possesses the controlling role. The values used for calculation were $u_L = 80 \cdot 10^{-9}$ m$^2$ V$^{-1}$ s$^{-1}$, $u_T = 20 \cdot 10^{-9}$ m$^2$ V$^{-1}$ s$^{-1}$, $u_R = 40 \cdot 10^{-9}$ m$^2$ V$^{-1}$ s$^{-1}$, $l_T = l_L = 0.01$ m, $c_L = 0.01$ *M*, $u_{BGC}$ = (1) $30 \cdot 10^{-9}$, (2) $50 \cdot 10^9$ and (3) $60 \cdot 10^{-9}$ m$^2$ V$^{-1}$ s$^{-1}$.

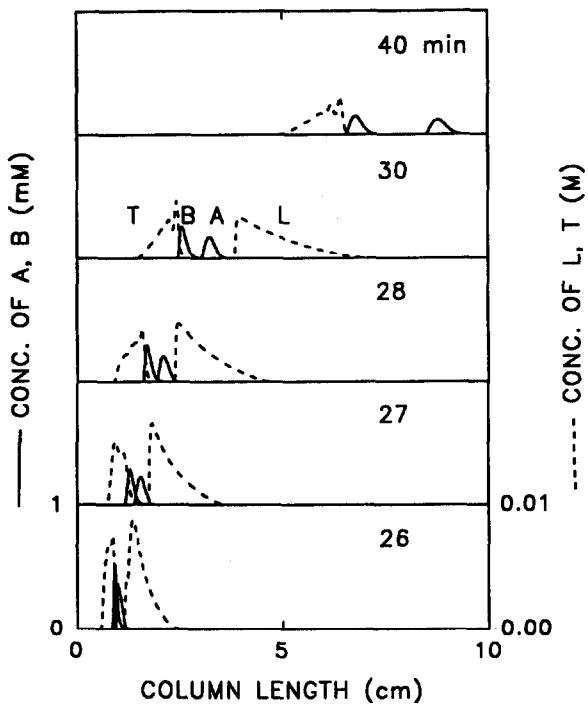


Fig. 19. Computer simulation of the separation of a pair of analytes A and B by the ITP–ZE combination of the BGE–S–BGE electrolyte system from Fig. 17. The isotachophoretic step was the same as shown in Fig. 8a. The concentration profiles shown correspond to the denoted time intervals. For the values used for calculations, see Table I. The rear part of the profile of the T zone is distorted owing to minor oscillations generated during the simulation.

which are 26.8 min for component A and 35.2 min for component B.

## CONCLUSIONS

The on-line combination of capillary ITP and CZE is a very important technique especially for the separation of complex biological fluids. The concentrating capabilities of ITP, which is used as the first separation step, are combined with the resolving power and detection sensitivity of CZE, thus allowing efficient determinations of trace components in complicated sample matrixes. Although the final step of such an analysis is performed in the zone electrophoretic mode, simple rules that hold for single zone electrophoretic analysis cannot be applied here directly. The reason is that the stack of zones introduced

into the zone electrophoretic step always involves some amounts of both leading and terminating zones. Thus, for a certain transient time, the ITP process survives and significantly affects the zone electrophoretic migration. The sample components leave the transient ITP stack gradually, depending on their mobilities, and hence each sample component starts its zone electrophoretic migration at a different time point and at a different column position. This brings about variations of migration times which are used for the qualitative evaluation of zone electrophoretic analyses and the magnitude of this effect depends on the electrolyte used for the zone electrophoretic step and on the amount of either the leader or terminator introduced into this second step. Moreover, if the mentioned amount is too large, some sample components may reach the detector being still stacked and thus not resolved.

The mathematical description presented in this paper provides a detailed insight into the processes that occur during the zone electrophoretic step for all possible types of electrolyte used, especially when the leader or the terminator is used directly as the background electrolyte. The theory allows one to predict the parameters necessary for a given analysis, especially the time when a sample component passes the detector (eqn. 7 or 20) or the position in the capillary where a component starts to migrate zone electrophoretically (eqn. 4 or 19). Based on this, the operating conditions and the amount of the leader and/or terminator introduced into the zone electrophoretic step can be selected so that the stacking effects are substantially reduced and controlled. The destacking process is illustrated by computer simulations that confirm also the values of individual parameters calculated by using the equations following from the theory presented here.

## SYMBOLS

$c_{i,j}$ concentration of substance $i$ in capillary $j$ or zone $j$
$i_j$ electric current density in capillary $j$
$l_L$ length of the leading zone in the preseparation capillary to be cut into the analytical one (T–S–T system)
$l_L^*$ value of $l_L$ reduced to the cross-section of the analytical capillary
$l_T$ length of the terminating zone in the analytical capillary (L–S–L system)
$p_{i,j}$ selectivity between substances $i$ and $j$
$S_1$ cross-section of the analytical capillary
$S_3$ cross-section of the preseparation capillary
$t$ time
$t_d$ time when the isotachophoretic plateau of the stacking zone in the analytical capillary disappears
$t_{X,e}$ time when substance X leaves the stack
$t_{X,r}$ time when zone X passes through the detector
$t_{z,r}$ time when the sharp boundary of the stacking zone passes through the detector
$t_0$ time when the entire zone of L has migrated into the analytical capillary (T–S–T system)
$u_X$ electrophoretic mobility of ion X
$u_{X,max}$ mobility of the ion X which is destacked just when passing through the detector (T–S–T system)
$u_{X,min}$ mobility of the ion X which is destacked just when passing through the detector (L–S–L system)
$v_{T-L}$ isotachophoretic velocity in the analytical capillary
$v_z$ velocity of the sharp boundary of the L–T transition zone
$v_1$ velocity of a single ion T in zone L
$v_2$ velocity of a single ion L in zone T
$x$ longitudinal coordinate
$x_d$ coordinate at which the isotachophoretic plateau of the stacking zone in the analytical capillary disappears
$x_r$ position of the detector
$x_{X,e}$ coordinate at which substance X leaves the stack
$x_z$ position of the sharp boundary of the L–T transition zone
$\kappa_L$ specific conductivity of the leading electrolyte in the analytical capillary (L–S–L system)
$\kappa_{L-T}$ specific conductivity of the L–T transition zone
$\kappa_T$ specific conductivity of the terminating electrolyte in the analytical capillary (L–S–L system)

$\kappa_z$ specific conductivity of the L–T transition zone at its sharp boundary
$\kappa_1$ specific conductivity of the terminating electrolyte in the analytical capillary (T–S–T system)
$\kappa_3$ specific conductivity of the leading electrolyte in the preseparation capillary (T–S–T system)
${}^t\sigma_X$ time-based variance of zone X

ACKNOWLEDGEMENT

This work was partly sponsored by the Swiss National Science Foundation.

REFERENCES

1 F.E.P. Mikkers, F.M. Everaerts and Th.P.E.M. Verheggen, *J. Chromatogr.*, 169 (1979) 1.
2 F.E.P. Mikkers, F.M. Everaerts and Th.P.E.M. Verheggen, *J. Chromatogr.*, 169 (1979) 11.
3 R.L. Chien and D.S. Burgi, *Anal. Chem.*, 64 (1992) 489A.
4 P. Gebauer, W. Thormann and P. Boček, *J. Chromatogr.*, 608 (1992) 47.
5 B. Gaš, J. Vacík and I. Zelenský, *J. Chromatogr.*, 545 (1991) 225.
6 S. Terabe, K. Otsuka, K. Ichikawa, A. Tsuchiya and T. Ando, *Anal. Chem.*, 56 (1984) 113–116.
7 J.W. Jorgenson and K.D. Lukacs, *Anal. Chem.*, 53 (1981) 1298.
8 F. Foret, L. Křivánková and P. Boček, *Capillary Zone Electrophoresis*, VCH, Weinheim, in press.
9 R. Aebersold and H.D. Morrison, *J. Chromatogr.*, 516 (1990) 79.
10 E. Kenndler and K. Schmidt-Beiwl, *J. Chromatogr.*, 545 (1991) 397.
11 G. Bondoux, P. Jandik and W.R. Jones, *J. Chromatogr.*, 602 (1992) 79.
12 S.E. Moring, J.C. Colburn, P.D. Grossman and H.H. Lauer, *LC · GC*, 8 (1989) 34.
13 A.C. Schoots, T.P.E.M. Verheggen, P.M.J.M. De Vries and F.M. Everaerts, *Clin. Chem.*, 36 (1990) 435.
14 Th.P.E.M. Verheggen, A.C. Schoots and F.M. Everaerts, *J. Chromatogr.*, 503 (1990) 245.
15 Ch. Schwer and F. Lottspeich, *J. Chromatogr.*, 623 (1992) 345.
16 V. Dolník, K.A. Cobb and M. Novotny, *J. Microcol. Sep.*, 2 (1990) 127.
17 F. Foret, V. Šustáček and P. Boček, *J. Microcol. Sep.*, 2 (1990) 229.
18 F. Foret, E. Szoko and B.L. Karger, *J. Chromatogr.*, 608 (1992) 3.
19 D.S. Stegehuis, H. Irth, U.R. Tjaden and J. Van Der Greef, *J. Chromatogr.*, 538 (1991) 393.
20 D.S. Stegehuis, U.R. Tjaden and J. Van Der Greef, *J. Chromatogr.*, 591 (1992) 341.
21 D. Kaniansky and J. Marák, *J. Chromatogr.*, 498 (1990) 191.
22 L. Křivánková, F. Foret and P. Boček, *J. Chromatogr.*, 545 (1991) 307.
23 F.M. Everaerts, J.L. Beckers and Th.P.E.M. Verheggen, *Isotachophoresis—Theory, Instrumentation and Applications*, Elsevier, Amsterdam, 1976.
24 G. Erikson, *Anal. Biochem.*, 109 (1980) 239.
25 J.L. Beckers and F.M. Everaerts, *J. Chromatogr.*, 508 (1990) 3.
26 J.L. Beckers and F.M. Everaerts, *J. Chromatogr.*, 508 (1990) 19.
27 L. Křivánková, F. Foret, P. Gebauer and P. Boček, *J. Chromatogr.*, 390 (1987) 3.
28 S. Hjertén, in G. Milazzo (Editor), *Topics in Biochemistry and Bioenergetics*, Vol. 2, Wiley, New York, 1978, pp. 89–128.
29 P. Gebauer and P. Boček, *J. Chromatogr.*, 267 (1983) 49.
30 P. Gebauer, L. Křivánková and P. Boček, *J. Chromatogr.*, 470 (1989) 3.
31 P. Boček, M. Deml, P. Gebauer and V. Dolník, *Analytical Isotachophoresis*, VCH, Weinheim, 1988.
32 M. Bier, O.A. Palusinski, R.A. Mosher and D. Saville, *Science*, 219 (1983) 1281.
33 R.A. Mosher, D.A. Saville and W. Thormann, *The Dynamics of Electrophoresis*, VCH, Weinheim, 1992.
34 R.A. Mosher, P. Gebauer, J. Caslavska and W. Thormann, *Anal. Chem.*, 64 (1992) 2991.
35 H. Weber, *Die Partiellen Differential-Gleichungen der Mathematik und Physik*, Vol. I, Friedrich Vieweg, Braunschweig, 1910, p. 503.
36 P. Gebauer and P. Boček, *J. Chromatogr.*, 320 (1985) 49.
37 V. Šustáček, F. Foret and P. Boček, *J. Chromatogr.*, 545 (1991) 239.